EFFECT OF INTERMEDIATED CHEMICAL COMPOUNDS NO ON THE HYBRID N_2O DECOMPOSITION UNDER PERIODIC FLOW REVERSAL CONDITIONS

Falk Lindner[1], Frank Platte[*+], David W. Agar[+], Stefan Turek[*]

[+)]*Chair of Reaction Engineering, Department of Biochemical and Chemical Engineering*
University of Dortmund, Emil-Figge-Str. 66, D-44227 Dortmund, Germany

[*)]*Institute of Applied Mathematics and Numerics, Chair of Mathematics III*
University of Dortmund, Vogelpothsweg 87, D-44227 Dortmund, Germany

Abstract

Hybrid homogeneous-heterogeneous reactions can arise in catalytic reactions carried out at elevated temperatures. In this work, hybrid N_2O decomposition is investigated at higher temperatures. Unsteady-state processes, such as the periodic flow reversal of fixed-bed reactors have a considerable impact on the way reaction behaviour develops within distributed systems. For the first time, we present a macrokinetic model that incorporates the influence of competing adsorption and desorption of the reactants on the catalyst, as well as the shift in the observed activation energy of the catalyst in the presence of NO. We show that NO can lead to a considerable change in behaviour of the hybrid reaction, which consequently results in different macroscopic reactor performance and demonstrate this phenomenon with the aid of selected bifurcation diagrams.

Keywords: Reaction Engineering, Modelling, Direct Dynamic Simulation, Flow Reversal, Hybrid Reaction

1. Introduction

Catalytic gas-phase reactions represent an important field of chemical engineering. Some such reactions, for example the intial functionalisation of hydrocarbon feedstocks, are operated at elevated temperature levels (T > 700 °C) so that apart from the desired heterogeneous catalytic reaction, homogeneous non-catalytic contributions may additionally arise which interact with the former (Galle, 2001, Veser, 2000) . Reactions exhibiting such coupled catalytic and homogeneous (thermal) contributions are often referred to as hybrid reactions. Compared to simple catalytic reactions, hybrid systems can lead to modified chemical reaction pathways and consequently to different product yields and selectivities (Galle, 2001). Another difference can be observed in the temperature distribution – hybrid reactions tend to give rise to higher temperature peaks and narrower reaction zones – since the homogenous contributions with their higher activation enrgies tend to be qualitatively faster. Regardless of whether these homogeneous contributions are desired or not, there is still a lack of models available to describe the pertinant interactions occurring. Since the heat and mass balances in a chemical reactor are coupled in a non-linear manner the prediction of whether or not and how a hybrid reaction may develop (Galle, 2001) is by no means simple. Even if simple independent macrokinetics for the distinct heterogeneous and homogeneous reaction steps which adequately describe the process are available,, this need not be true for the coupled reaction. In other words: the macrokinetics for the

[1] Ccorresponding author. Tel.: +49 (0) 231 755-2673; fax: +49 (0) 231 755-2311.
Email- address: falk.lindner@bci.uni-dortmund.de (F. Lindner)

hybrid reaction is almost never simply the sum of the macrokinetics for the heterogeneous and homogeneous contribtuions. In this context, unsteady-state processes, such as the reverse flow reactor (rfr) and the loop reactor are of interest as a powerful diagnostic tool (Nalpantidis et. al, 2006, Mangold et al., 1999) for analysing the behaviour of hybrid reaction systems. Due to their complex dynamics, it is believed that unsteady-state processes allow for greater resolution and more discriminating insights into the chemical and physical interactions. In conjunction with system analysis techniques, such as bifurcation analysis, dynamic reactor operation it is a useful technique for studying complex reactor/reaction behaviour.

Salinger and Eigenberger (1996a,b) have analysed the parallel oxidation of propane and propene in an rfr. They found a different number of possible multiple steady-states depending on the composition of the feed gas used. Mangold et al. studied a parallel reaction system in a loop reactor (1999). They found a change in the rate of the temperature front propagation, depending on the difference in activation energy of the individual reactions. In the work of Khinast and Luss, a cooled reverse flow reactor exhibited complex behaviour which could be 'tuned' using the cooling rate (1998). Ciambelli et al. found oscillating and non-oscillating regions for different feed gas concentrations (1999), but in contrast to the previously mentioned groups, they studied only the local activities on the catalyst surface. Kapteijn et al. detected interesting shifts in the observed activation energy for various types of catalysts (e.g. Fe, Mn) in the presence of oxidising intermediate species (e.g. CO, NO) (1997).

The work presented in this paper is based on earlier research done by Nalpantidis, Platte et al. who studied the hybrid N_2O decomposition of in an rfr with segmented catalyst/inert fixed-bed structures (2006). As an extension to their work, we have developed a model which additionally accounts for the generationn of an intermediate chemical species and its influence on the course of the hybrid reaction. We identified NO as being a chemical species that potentially affects the reaction pathway for both the heterogeneous and homogeneous reaction. For the first time, we present a global macrokinetic model that incorporates both the influence of competing adsorption and desorption steps due to NO and a shift of the observed activation energy of the catalyst due to NO. We will show that NO can exert a considerable influence on the hybrid reaction, resulting in distinct modes of macroscopic reactor behaviour. We will illustrate this with the aid of selected bifurcation diagrams.

We utilised the directed dynamical simulation (dds) in combination with bifurcation analysis method, as published previously by our group (Nalpantidis et al. 2006).

2. From micro to macrokinetics

In this chapter, we present a survey of the chemical background of hybrid N_2O decomposition. This overview serves as basis to justify the mathematical model discussed in the following section. The following schematic illustration gives a brief description of the processes taking place in the vicinity of the catalyst surface

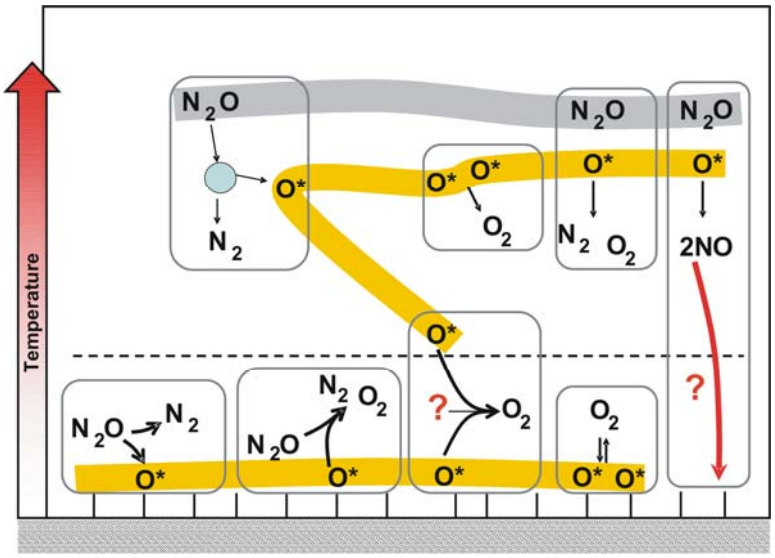

Fig. 1: *Chemical reactions in the gas bulk phase and in the vicinity of the catalytic surface*

As one can see from Fig. 1, the species NO, which plays a key role in our work, is only formed in the gas-phase, but nevertheless has a strong influence on the behaviour of solid catalytic phase. Previous work of Kapteijn et al. (1997) clearly showed that the species NO may have a strong influence on chemical reactions taking place on the solid catalytic surface. In particular, it was observed that NO has a significant influence on the N_2O decomposition if a Fe-ZSM-5 catalyst was used.

At the molecular level, the following reactions might be considered to occur on the catalyst's surface (Kapteijn, 1997, Galle, 2001):

$$N_2O \leftrightarrow N_2O^* \quad (2\text{-}1)$$

$$O^{\cdot} \leftrightarrow O^* \quad (2\text{-}2)$$

$$NO \leftrightarrow NO^* \quad (2\text{-}3)$$

$$2\,N_2O^* \rightarrow 2\,N_2^* + O_2^* \quad (2\text{-}4)$$

$$N_2O^* + O^* \rightarrow N_2^* + O_2^* \quad (2\text{-}5)$$

$$N_2O + O^* \rightarrow N_2^* + O_2^* \quad (2\text{-}6)$$

$$N_2O^* + O^{\cdot} \rightarrow N_2^* + O_2^* \quad (2\text{-}7)$$

$$NO^* + O^* \rightarrow NO_2^* \quad (2\text{-}8)$$

$$NO^* + O^{\cdot} \rightarrow NO_2^* \quad (2\text{-}9)$$

$$N_2^* \leftrightarrow N_2 \quad (2\text{-}10)$$

$$O_2^* \leftrightarrow O_2 \quad (2\text{-}11)$$

$$NO_2^* \leftrightarrow NO_2 \quad (2\text{-}12)$$

The asterisk denotes that a compound is adsorbed on the surface. Equations (2-1), (2-2) and (2-3) describe the adsorption of the different species present on the solid surface of the catalyst. This adsorption is assumed to be of a physical nature, i.e. the bonding of the molecules on the solid surface is only weak. Furthermore, all adsorptions are treated as reversible steps. Moreover, the equations (2-4) to (2-8) represent chemical reactions which might take place on the solid surface. In contrast to the equations describing the adsorption of the different species, these chemical reactions are treated as being irreversible. Lastly, the equations (2-10), (2-11) and (2-12) represent the desorption of the adsorbed product-species from the solid surface.

It should be noted that from a thermodynamic point of view, the chemical compound NO_2 is not stable at elevated temperatures and dissociates (Walz, 2000), but this has no influence on the model presented in the next chapter.

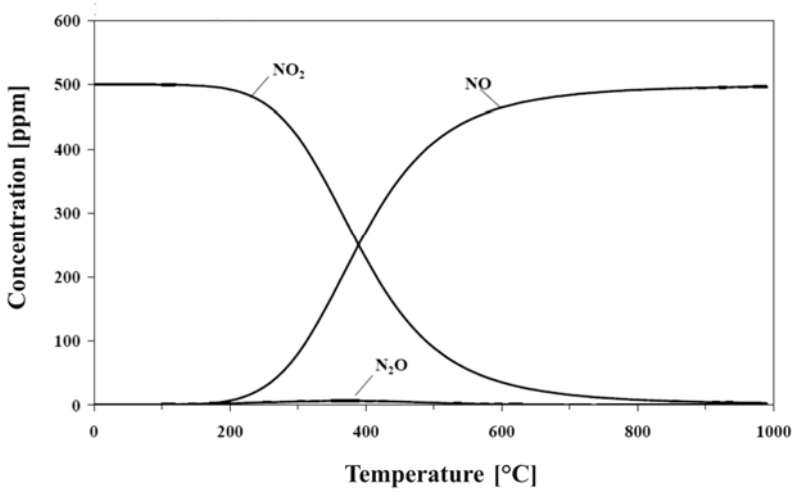

Fig. 2: *Temperature dependent equilibrium of NO_2 und NO. At elevated temperature (above 650 °C) almost no NO_2 is present*

A few simplifying assumptions have been made with respect to the model. Firstly, the formation of oxygen is treated as the rate-limiting step. This means that the residence time of adsorbed oxygen is very high compared to the other chemical species involved and thus that it may block the catalyst's active surface sites. Secondly, as can be seen in equations (2-8) and (2-9), no distinction is drawn between the Langmuir-Hinshelwood-mechanism and the Elay-Rideal-mechanism. Thirdly, as mentioned above, the formation of NO according to the chemical reaction

$$N_2O + O^{\cdot} \rightarrow 2\,NO \qquad (2\text{-}13)$$

is considered to occur in the gas phase only. However, its influence on the catalyst surface is strong (see above) and this feature will be treated in detail in the next section.

3. Mathematical model

This section presents the mathematical model describing the reaction mechanism given above. The model derived here is based on previous work of Galle (2001) in which the TC-model (TC: thermal-coupling) was first used. In Galle's work, a pseudo-homogeneous model comprising one mass balance and one energy balance was used. The kinetic equation – which couples the two balance equations and describes the reaction rate of the hybrid reaction – consisted of two independent terms: one for the homogeneous reaction rate and the other one for the catalytic reaction rate. The latter term also accounted for a mass transport limitation through the boundary layer.

$$\Rightarrow r^{TC}\left(T, c_s\right) = \left[k^{hom}\left(T\right) + \frac{a_v \cdot \beta \cdot k^{het}\left(T\right)}{a_v \cdot \beta + k^{het}\left(T\right)} \right] \cdot c_S \qquad (3\text{-}1)$$

A comparison of the experiments conducted in a technical-scale reactor in our laboratory and simulations based on this simple TC-model exhibited a fairly good agreement correlation with respect to the temperature profile (Nalpantidis et al., 2006).

In this paper, our goal is to also account for an intermediate species, which might influence the reaction mechanism of the N_2O decomposition. NO would seem to be a promising candidate for this purpose (cf. 2-1 – 2-12). An extension of the TC-model is necessary due to the additional phase which must now be considered. Thus, the advanced/augmented model must include mechanisms for the formation and adsorption of NO. Models which account for thermal and chemical coupling are denoted TCC-models.

From a mathematical point of view, this model consists of equations with different reaction rate terms. Two independent equations for the reaction rates of nitrous oxide and nitric oxide were used. This makes it possible to account for the formation of both nitrous oxide and nitric oxide independently of one another.
The model can be described with the following equations:

$$r_{N_2O}^{hyb}(T,c_{N_2O},c_{NO}) = \left(\frac{a_v\beta \cdot k_{N_2O}^{het}(T,c_{NO}) \cdot e^{\left(-\frac{E_{A,N_2O}^{het}+bc_{NO}}{RT}\right)}}{a_v\beta + k_{N_2O}^{het}(T,c_{NO}) \cdot e^{\left(-\frac{E_{A,N_2O}^{het}+bc_{NO}}{RT}\right)}} (1-\theta \cdot c_{NO}) + (1-\phi) \cdot k_{0,N_2O}^{\hom}(T) e^{\left(-\frac{E_{A,N_2O}^{\hom}}{RT}\right)} \right) \cdot c_{N_2O} \tag{3-2}$$

$$\mathrm{k}_{\mathrm{N_2O}}^{\mathrm{het}}(\mathrm{T},\mathrm{c}_{\mathrm{NO}}) = \mathrm{k}_{0,\mathrm{N_2O}}^{\mathrm{het}}(\mathrm{T}) \cdot (1-\delta \cdot \mathrm{c}_{\mathrm{NO}}) \tag{3-3}$$

$$r_{NO}^{hyb}(T,c_{N_2O},c_{NO}) = \phi \cdot k_{0,NO}(T) e^{\left(-\frac{E_{A,NO}}{RT}\right)} \cdot (c_{N_2O} - \varphi \cdot c_{NO}) \tag{3-4}$$

Equation (3-2) represents the core of the kinetic model. Equation (3-3) contains a modified Arrhenius expression for the heterogeneous reaction. In (3-4) the mathematical description of the formation and sorption of NO is reflected.

The concept behind the model is as follows: adsorbed oxygen and nitrous oxide on the catalytic surface block the catalyst's free sites. The high concentrations of both adsorbed oxygen and nitric oxide on the catalyst thus reduce the decomposition rate of nitrous oxide. The formation of nitrogen dioxide is not considered further in this model. This means that there is a competition between the adsorbed oxygen and the nitric oxide created in the gas phase with respect to the blockage of the free catalytic sides.

There is a nitrous oxide concentration threshhold above which the decomposition rate does not increase. In terms of the model, high concentration of nitrous oxide in the gas phase can enhance the decomposition rate of this species – but only up to a specific level.
The model was derived on the basis of several earlier publications (Pikios et al. 1977; Schlosser, 1972; Ciambelli et al., 1999; Galle, 1999; Kapteijn et al., 1997)). Certainly other mathematical models might be envisaged and alternatives can be found in (Lindner, 2005).

The dependence of the observed activation energy for N_2O-decomposition on the NO - concentration in the gas phase has been taken into account by many researchers Pikios et al. 1977; Schlosser, 1972; Ciambelli et al., 1999).
Two different relationships have been suggested.

$$E = E_0 + b \cdot c \tag{3-5}$$

$$E = E_0 \cdot b \cdot c \tag{3-6}$$

Pikios and Luss (1977) suggest equation (3-5), while equation (3-6) has been devised by Ciambelli et al. (1999). Pikios and Luss (1977) investigated the influence of the heterogeneity of the solid catalyst active sites and presented a corresponding mathematical model, which predicted kinetic oscillations for realistic parameter values. A dependence of the activation energy for a chemical reaction on the surface coverage of a chemical compound was a component of this model. While Pikios and Luss (1977) presented a very general mathematical model which may lead to kinetic oscillations, Ciambelli (1999) and co-workers investigated the decomposition of nitrous oxide catalysed by a Cu-ZSM-5 catalyst. They proposed a change in the catalyst's state of oxidation and they also assumed a non-constant activation energy. In contrast to Pikios and Luss (1977), they proposed a dependence of the activation energy on the catalyst's degree of reduction.

From our point of view, however, equation (3-6) does not describe the problem correctly, because for b=0 the value of the activation energy also becomes 0. Factor b accounts for the influence of the adsorbed nitric oxide on the activation energy. The higher the value of b, the stronger the influence of the adsorbed nitric oxide.

Furthermore, a transport limitation for mass transfer to the catalytic surface has been discussed by Galle (2001). The model for this transport resitance can be derived from a mass balance around the catalyst (Salinger and Eigenberger, 1996a):

$$0 = a_v \cdot \beta \cdot \left(c_g - c_s\right) - k^{het}(T) \cdot c_s \tag{3-7}$$

$$\Leftrightarrow c_s = \frac{a_v \cdot \beta \cdot c_g}{k + a_v \cdot \beta} \tag{3-8}$$

$$\Rightarrow r^{het}(T, c_s) = k^{het}(T) \cdot c_s = \frac{a_v \cdot \beta \cdot k^{het}(T)}{a_v \cdot \beta + k^{het}(T)} \cdot c_g \tag{3-9}$$

Equation (3-9) means that the reaction rate cannot achieve infinite values, i.e. the reaction rate is limited to a finite value. The values for the various parameters used in this article are given in the tables.

Furthermore, we introduced two dimensionless numbers that help us in assessing to what degree the heterogeneous and homogeneous reactions are coupled. First of all we define the number Pn:

$$Pn = \frac{r^{hom}(T, c)}{r^{het}(T, c)} \tag{3-10}$$

that describes the local ratio between the homogeneous and the heterogeneous rate. Pn is unity when the individual reactive contributions are of the same magnitude, while Pn approaches zero or infinity when one of the reactions dominates. Pn serves only as an auxiliary value required for the second non-dimensional number Hyb.

$$Hyb = \exp\{-(\log_{10} Pn)^2\} \tag{3-11}$$

The Hyb-number has the following properties. Hyb is also unity for equal homogeneous and heterogeneous reaction contributions, but in contrast to Pn, Hyb converges to zero if one - regardless

which - reaction dominates. Fig. 4 and Fig. 5 illustrate the behaviour of Pn and Hyb based on the kinetics described in (3.9).

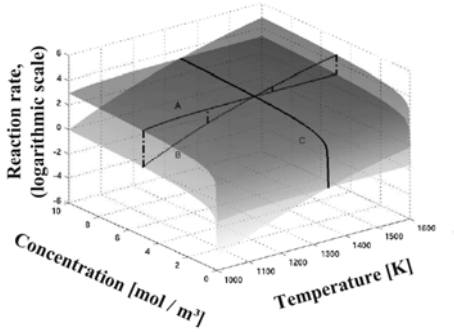

Figure 4: *Reaction rate (on a logarithmic scale) for the decoupled homogeneous and heterogeneous reaction rate depending on concentration and temperature*

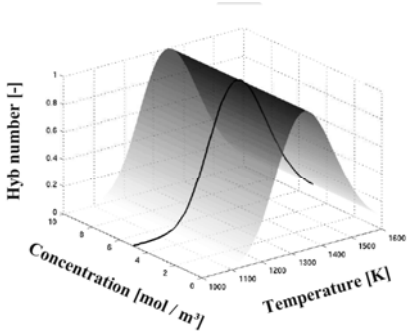

Figure 5*: Distribution of the Hyb number for the chemically uncoupled hybrid N2O decomposition depending on concentration and temperature*

Direct calculation of cyclic steady-states

The operating principles of an rfr are well-known. By simultaneously opening one valve pair whilst closing the other or vice versa, the flow direction and inlet-outlet-arrangement is reversed. The main advantage of the periodic flow reversal concept is that a hot reaction zone is trapped in the centre of the reactor fixed-bed surrounded by two cold peripheral zones. Although this type of reactor with regenerative heat exchange was first proposed in the nineteen thirties it first became well-known through the extensive work of Matros (1996).

We chose a simple three-equation model to describe the distribution of temperature and concentration in the reactor. The model comprises two balance equations, one a pseudo-homogeneous energy balance, the other a mass balance. Both are usually partial differential equations (PDEs) in time and (one-dimensionally) in space. Due to the dominating influence of the heat balance, the mass balance is assumed to be in pseudo-steady-state. Nevertheless, since the gas phase composition is coupled to that of the solid catalyst via the reaction term, it also implicitly depends on time. The resulting system can be represented by the following expressions:

$$\varepsilon(\rho c_P)_g + (1-\varepsilon)(\rho c_P)_s \frac{\partial T}{\partial t} = \lambda_{eff} \frac{\partial^2 T}{\partial z^2} - (\rho c_P)_g v \frac{\partial T}{\partial z} + \frac{k}{r}(T - T^{amb}) + (-\Delta H_r) r_{N_2O}^{hyb} + (-\Delta H_r) r_{NO}^{hyb} \tag{3-12}$$

$$0 = D_{eff} \frac{\partial^2 c_{N_2O}}{\partial z^2} - v \frac{\partial c_{N_2O}}{\partial z} - r_{N_2O}^{hyb}(T, c_{N_2O}, c_{NO}) \tag{3-13a}$$

$$0 = D_{eff} \frac{\partial^2 c_{NO}}{\partial z^2} - v \frac{\partial c_{NO}}{\partial z} - r_{NO}^{hyb}(T, c_{N_2O}, c_{NO}) \tag{3-13b}$$

For a spatial boundary condition we used the usual Danckwerts boundary conditions (Nalpantidis et al. 2006). Following flow-reversal, the convective terms in (3-12) and (3-13) change their signs and the spatial boundary conditions are switched. The relevant physical data employed can be found in table 1.

Table 1 Physical data used in the mathematical rfr model

ε	[-]	0.69	R	[J/(mol K)]	8.3143
ρ_s	[kg/m^3]	1645	$k^{het}_{N_2O}$	[1/s]	$3 \cdot 10^8$
ρ_g	[kg/m^3]	0.486	$k^{hom}_{N_2O}$	[1/s]	$4.4 \cdot 10^{11}$
$c_{p,s}$	[J/(kg K)]	840.0	k^{hom}_{NO}	[1/s]	$4.4 \cdot 10^{11}$
$c_{p,g}$	[J/(kg K)]	1093.0	E^{het}_{A,N_2O}	[J/mol]	150000
T^{amb}	[K]	300	E^{hom}_{A,N_2O}	[J/mol]	250000
λ_{eff}	[W/(m K)]	0.85	$E_{A,NO}$	[J/mol]	250000
v	[m/s]	0.4	L	[m]	1.5
$\Delta H_{r,N_2O}$	[J/mol]	81600	A	[W/(m^2 K)]	91.0
$\Delta H_{r,NO}$	[J/mol]	392000	$\Delta t_{cyc.}$	[s]	300, 500
D_{eff}	[m^2/s]	0.00691	a_v	[1/m]	1100
T^0	[K]	300	β	[m/s]	0.18

(The parameters λ_{eff} and D_{eff} are due to the fact that a homogeneous model is being used for the simulation.)

Simulation techniques

The defining system of PDEs presented above consists of one energy balance coupled with two mass balances for the two chemical species NO and N_2O. In the following, we describe the most important numerical aspects of the simulation code implemented in Matlab 7.0 (R14).

Earlier research clearly demonstarted that the direct calculation approach (sometimes also referred to as Direct Dynamical Simulation (dds)) is far more efficient than a simple dynamic simulation – if only cyclic steady-states are of major interest (Salinger and Eigenberger, 1996a). In particular, this can be said to be true for the case of parameter studies in which hundreds of cyclic steady-states are to be calculated. We had to carry out such parameter studies to genreate the ignition-extinction bifurcation diagrams sought. To save disc storage and processing time we restricted the global discretisation to a single half-cycle and assumed the symmetry of temperature profiles as a boundary condition in time.

The global discretisation of the energy balance is the crucial step. We chose a two-dimensional, equidistant spaced grid to discretise over the reactor length $0 < z < L$ and switching time $0 < t < \Delta t_{cyc}$. We applied a modified Finite Difference grid (FD) published earlier (Nalpantidis et al., 2006) . The CN - CDS/LUDS approach presented is roughly second order in both space and time. The result of the global discretisation is a large – and due to the reaction terms – coupled and non-linear system of equations.

Since the ignition-extinction diagrams exhibit turning points in which simple parameter continuation tracking algorithms would fail, we applied Keller's pseudo-arc-length-continuations technique in the same way as described in (Doedel, 2000).

4. Results and discussion

We identified the model parameter ϕ as having a strong influence on the overall macroscopic behaviour. Fig. 6 shows the complex ignition-extinction behaviour depending on N_2O feed-concentration and the NO formation parameter ϕ. By virtue of to the cut-plane (c_{N2O} = 0.78 mol/m³) section it can be recognised that the ignited state significantly changes depending on ϕ and that for a small ϕ interval a second-order bifurcation arises. For c_{N2O} = 0.78 mol/m³ experimental data is also available.

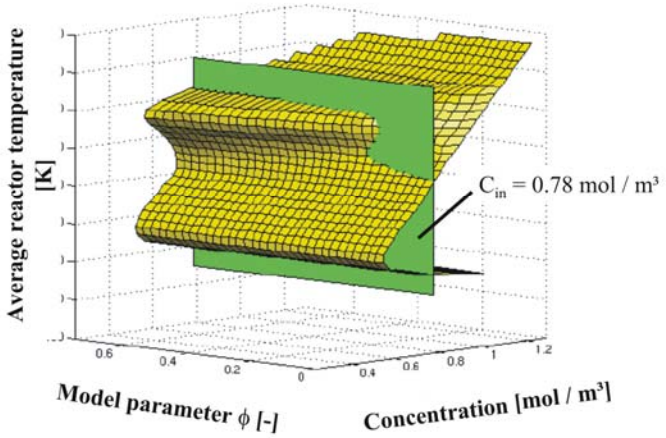

Fig. 6: *Complex ignition-extinction behaviour depending on N_2O feed-concentration and NO formation parameter ϕ .*

By varying the parameter ϕ, one can greatly influence the formation of nitric oxide. The higher the value of the parameter, the more nitric oxide is generated. As mentioned above, an assumption in the presented model is the dependence of the activation energy of the nitrous oxide decomposition reaction on the concentration of the nitric oxide in the gas phase. The higher the concentration of nitric oxide in the gas phase, the higher the value of the activation energy of the nitrous oxide decomposition reaction. A glance at Fig. 6 reveals why the bifurcation behaviour shifts from three to five branches. The higher the activation energy of the nitrous oxide decomposition reaction, the higher the reaction temperature required to maintain the decomposition reaction. Furthermore, the higher the reaction temperature, the larger the influence of the homogeneous nitrous oxide decomposition. According to this interpretation, the switch from the three branch bifurcation system to five branch system occurs on account of the increasing influence of the homogeneous decomposition reaction at higher reaction temperatures. Variations of the model parameter b did not display such a significant influence on the system's behaviour. In Fig.7 four ignited steady states are depicted for a switching time of 500 seconds. The first and third columns are dynamically unstable, whereas the second and fourth column represent stable solutions.

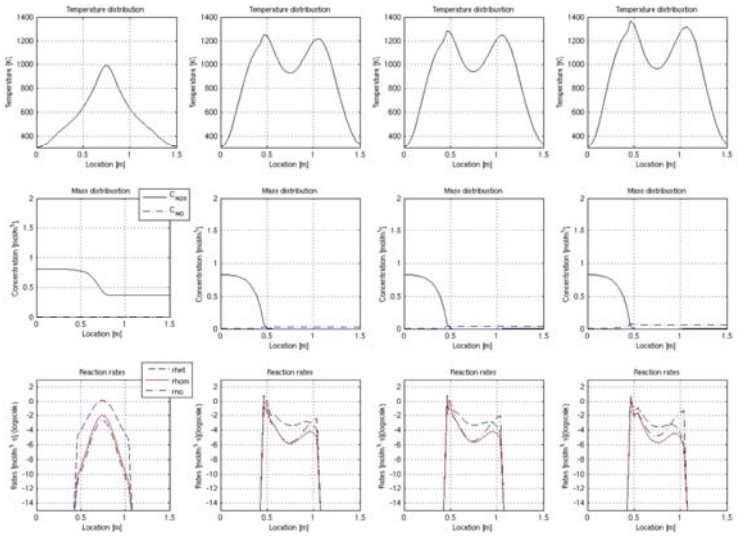

Fig. 7: *Four ignited steady-states. The first to third rows depict heat distribution, mass distribution and reaction rates. The first and third columns are dynamically unstable, whereas the second and fourth column represent stable solutions*

Another interesting point is of course the comparison of the simulated data with data obtained experimentally. During some experiments we observed a significant difference between the predicted temperature distribution and the measured result. Since many experiments could be validated with a simple TC-model it is believed that a chemical coupling due to NO is the reason for the observed deviations. In the following three cases, the simulations are compared to an experiment with medium feed concentration (c_{N_2O} = 0.78 mol/m³) and medium switching time (Δt_{cyc} = 360 s) in order to estimate the extent of a possible chemical coupling. The relevant kinetic values can be found in table 1.

Table 2*: Kinetic values for three different cases*

CASE		**I**	**II**	**III**
δ	$[\,m^3/mol\,]$	0.2	0.2	0.2
b	$[\,(J\cdot m^3)/mol\,]$	20000	20000	20000
θ	$[\,m^3/mol\,]$	1	1	1
ϕ	[-]	0.0	0.2	0.2
φ	$[\,m^3/mol\,]$	0.1	0.1	0,1
k	$[\,W/(m^2\cdot K)\,]$	40	40	40

Remarkably, the cases II and III have identical kinetic parameters although the results appear very different. The explanation for this is to be found in the second order bifurcation depicted in Fig. 6.

CASE I

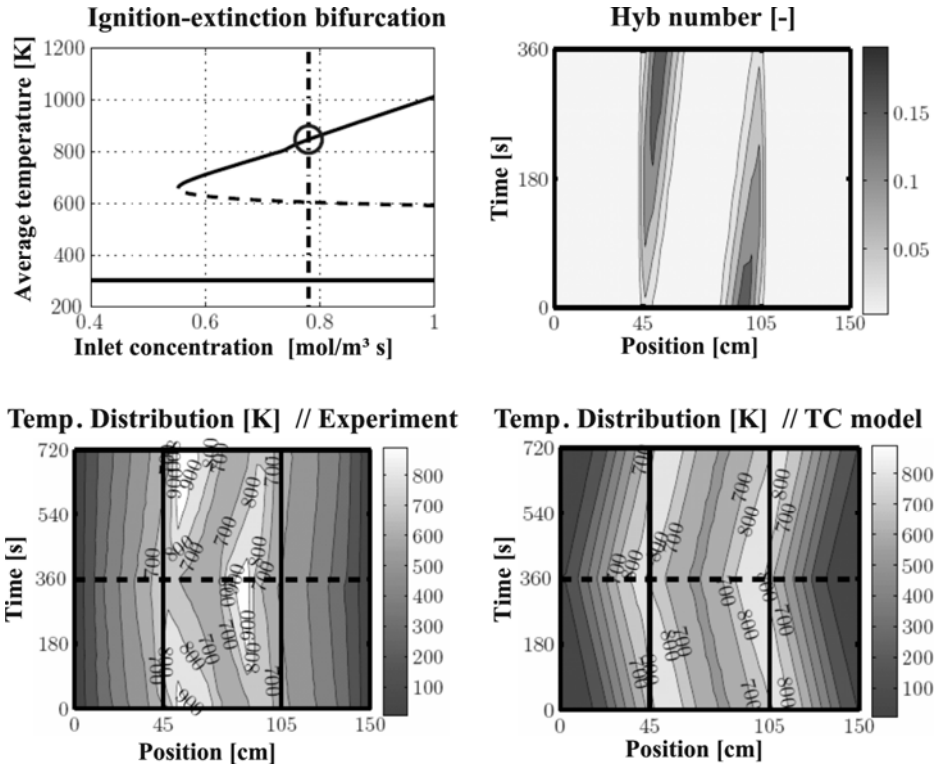

Fig. 8: *Case I, no chemical coupling: Ignition-extinction bifurcation (upper left), behaviour of the Hyb-number (upper right) and comparison of the temperature distribution for experiment (lower left) and simulation (lower right)*

Case I is depicted in Fig. 8. For this case the model parameter ϕ was set to zero, which means that there is no chemical coupling between the heterogeneous and homogeneous reactions. The bifurcation diagram shows three intersections with the c_{N_2O} = 0.78 mol/m³, which is the standard behaviour pattern for individual independent reactions or for the hybrid reaction found with the TC model. Indeed, choosing ϕ=0 leads to a standard TC-model since NO is not formed. The two lower diagrams illustrate the temperature distribution for the experiment and simulation. A significant under-prediction of temperature values is observed (see above). The upper right diagram illustrates how the parameter Hyb behaves during the half-cycle in both space in time. Rather small values of Hyb are found (Hyb< 0.15), which is a result of the assumptions made in the TC-model. The distribution of Hyb is nearly mirror-symmetric but only the reaction zone in the vicinity of z= 0.45 metres is of importance.

CASE II

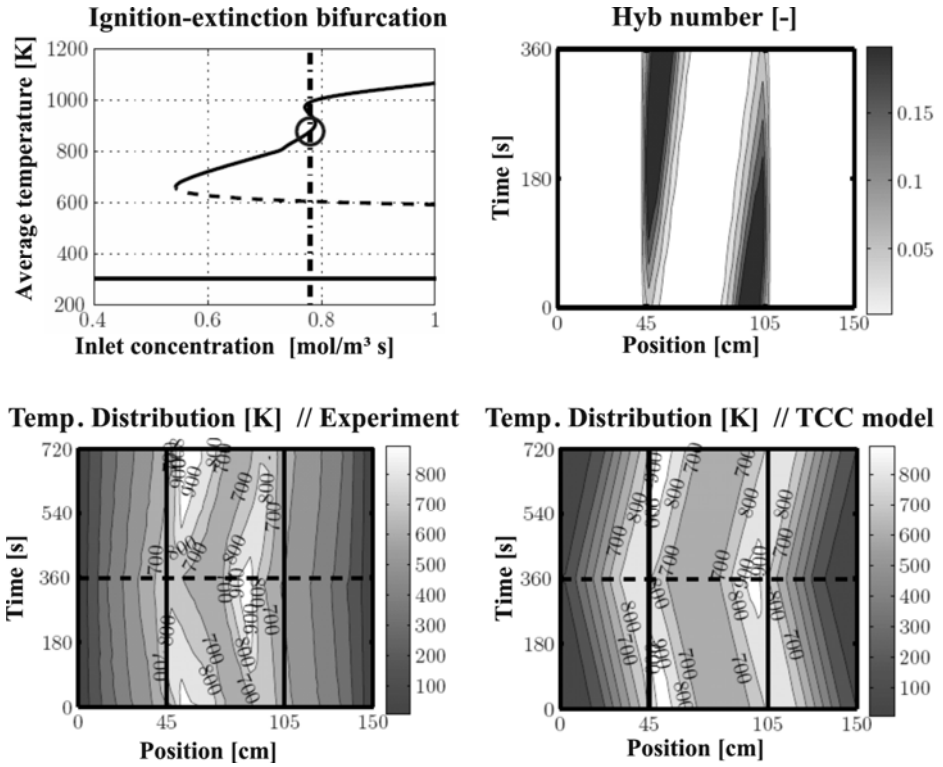

Fig. 9: *Case II, low chemical coupling: Ignition-extinction bifurcation (upper left), behaviour of the Hyb-number (upper right) and comparison of the temperature distribution for experiment (lower left) and simulation (lower right)*

Case II is depicted in Fig. 9. For this case the model parameter ϕ was set to 0.2, which means that a significant amount of NO is being generated in the homogenous reaction. The bifurcation diagram once again shows three intersections with c_{N_2O} = 0.78 mol/m³ but for larger values of c_{N_2O} the gradient changes. The two lower diagrams show the temperature distribution for the experiment and simulation. Although the isotherms do not coincide perfectly, the qualitative behaviour is by far better than in case I. The values are predicted more accurately, as can be seen in particular from the size and position of the T=900 K isotherm. The upper right diagram illustrates again how Hyb behaves during the half-cycle in space and in time. Once again, a mirror-symmetric distribution of Hyb is observed, although the values are much larger than in case I.

CASE III

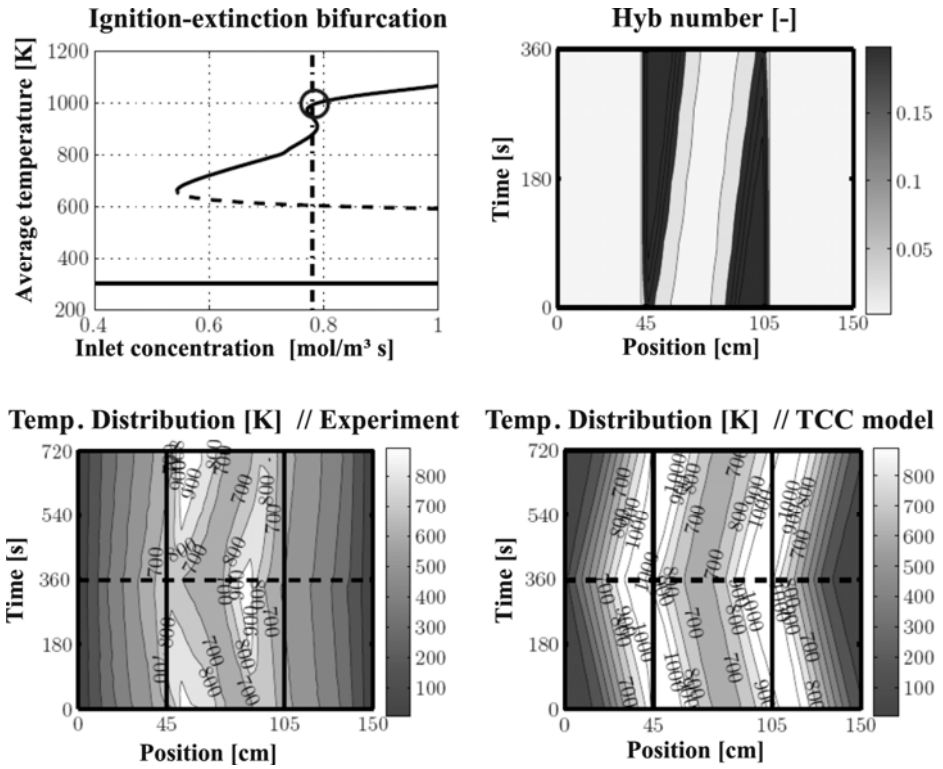

Fig. 10: *Case III, high chemical coupling: Ignition-extinction bifurcation (upper left), behaviour of the Hyb-number (upper right) and comparison of the temperature distribution for experiment (lower left) and simulation (lower right)*

Case III is depicted in Fig. 10. In this case the model parameter ϕ was also set to 0.2, just as in case II. Nevertheless the solution is different. The bifurcations diagram now exhibits five intersections with c_{N_2O} = 0.78 mol/m³. The location of case III is highlighted by the circle. In fact case III is another ignited solution coexisting with case II. However, inspection of the temperature distribution for the experiment and simulation enables one to conclude that this simulation case III is not an appropriate description of the experiment, since temperatures are considerably over-predicted . The upper right diagram again illustrates how Hyb behaves during the half-cycle in space and in time. A mirror-symmetric distribution of Hyb is present. The values are even higher than for case II.

5. Conclusion

A mathematical model has been presented which takes into account both the decomposition of nitrous oxide (N_2O) as well as the formation of nitric oxide (NO) as a chemical compound with a potentially large influence on the nitrous oxide decomposition reaction. The elaborated model accounts for both a competitive adsorptions/desorption effect of NO as well as a change of the catalyst's observed activation energy. As in earlier work, the fast and robust direct dynamic simulation based on global discretisation in combination with Keller's pseudo arc length path continuation method was used as the solution procedure. Values of the parameters ϕ and b reflecting the rate of NO generation and sensitivity of observed activation energy were examined. It could be demonstrated clearly that the formation of nitric oxide leads to a qualitatively distinct system behaviour as can be appreciated in the bifurcation diagrams. Furthermore, the influence of nitric oxide on the reactor temperature as well as on

the “hybridicity” of the decomposition reaction has been elucidated. For given experimental data we were able to estimate the degree of chemical coupling for the hybrid N_2O decomposition. The concept of exploiting the improved resolution offered by dynamic reactor operation to yield clear qualitative phenomena for model discrimination was thus validated satisfactorily.

6. Literature

Ciambelli, P., Di Benedetto, A., Pirone, R., and Russo, G., 1999. Mathematical modelling of self-sustained isothermal oscillations in N_2O decomposition on Cu-ZSM5, Chemical Engineering Science 54, 2555-2559.

Doedel, E., and Tuckermann, L.S., 2000. Numerical methods for bifurcation problems and large-scale dynamical systems. Springer, New York.

Lindner, F., 2005. Theoretische Untersuchung des Stabilitätsverhaltens gekoppelter chemischer Reaktionen in Festbettreaktoren, Diploma thesis, University of Dortmund.

Galle, M., 2001. Hybride homogene und heterogene Reaktionsführung in Hochtemperatursystemen am Beispiel der Lachgaszersetzung. PhD thesis, University of Dortmund.

Kapteijn, F., Marban, G., Rodriguez-Mirasol, J., and Moulijn, J.A., 1997. Kinetic Analysis of the Decomposition of Nitrous Oxide over ZSM-5 ,Catalysts, Journal of Catalysis 167, 256-265.

Khinast, U., Gurumoorthy, A., and Luss, D., 1998. Complex dynamic features of a cooled reverse-flow reactor. A.I.Ch.E.J. 44, 1128.

Mangold, M., Klienle, A., Gilles, E.D., Richter, M., and Roschka, E. 1999. Coupled reaction zones in a circular loop reactor. Chemical Engineering Science 54, 2597–2607.

Matros, Y.S., Bunimovich, G.A., 1996. Reverse-flow operation in fixed-bed catalytic reactors. Catalysis Reviews in Science and Engineering 38, 1–68.

Nalpantidis, K., Platte, F., Agar, D.W., and Turek, S., 2006. Elucidation of Hybrid N_2O decomposition using axially structured catalyst in reverse flow reactor, Chemical Engineering Science 61, 3176–3185.

Pikios, C.A., and Luss, D. 1977. Isothermal concentration oscillations on catalytic surfaces. Chemical Engineering Science 32, 191–194.

Salinger, A.G., Eigenberger, G., 1996b. The direct calculation of periodic states of the reverse flow reactor - I. methodology and propane combustion results. Chemical Engineering Science 51, 4903–4913.

Salinger, A.G., Eigenberger, G., 1996b. The direct calculation of periodic states of the reverse flow reactor - II. multiplicity and instabiliy. Chemical Engineering Science 51, 4915–4922.

Schlosser, E.G., 1972. Heterogene Katalyse. Verlag Chemie, Weinheim.

Veser, G., and Frauhammer, J., 2000. Modelling steady state and ignition during catalytic methane oxidation in a monolith reactor. Chemical Engineering Science 55, 2271–2286, 2000.

Walz, C., 2000. NOx-Minderung nach dem SCR-Verfahren: Untersuchungen zum Einfluß des NO_2 -Anteils. Ph.D. thesis, University of Karlsruhe.